THE JOURNAL OF PHYSICAL CHEMISTRY C

Article

pubs.acs.org/JPCC

Photocatalytic Decomposition of Methyl Formate over TiO_2-Supported Pt Metals

Gábor Schubert, Tamás Bánsági, and Frigyes Solymosi*

MTA-SZTE Reaction Kinetics and Surface Chemistry Research Group, University of Szeged, Rerrich Béla tér 1, H-6720 Szeged, Hungary

ABSTRACT: The photoinduced vapor-phase decomposition of methyl formate was investigated on pure and on Pt-metals-promoted TiO_2. Infrared spectroscopic studies revealed that illumination induced the dissociation of molecularly adsorbed methyl formate to formate on pure TiO_2 even at ~186 K. This process is indicated by the appearance of the absorption band at 1580−1590 cm^{-1} due to asymmetric stretch of formate species. The extent of the dissociation is increased with the time of irradiation. Deposition of Pt metals on TiO_2 only slightly influenced this process. The photocatalytic decomposition of methyl formate vapor on pure TiO_2 occurred to only a limited extent at 300 K, but the deposition of Pt metals on TiO_2 appreciably enhanced the extent and the rate of photodecomposition. Nevertheless the photocatalytic reaction of methyl formate proceeded more slowly compared to that of formic acid on the same catalysts, and produced more CO. Addition of H_2O to the methyl formate decreased the CO/H_2 ratio by a factor of 4. When the bandgap of TiO_2 support was lowered by N-doping from 3.02 to 1.98 eV, the photocatalytic activity of metal/TiO_2 catalysts appreciably increased, and the decomposition of methyl formate was observed even in visible light.

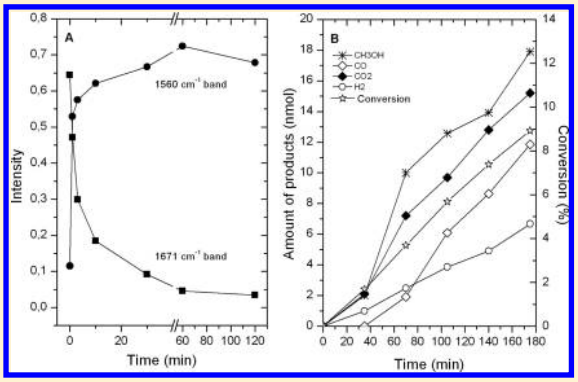

1. INTRODUCTION

A great effort has been made in the past decade to produce H_2 possibly free of CO. As a source of H_2 the most suitable compounds are ethanol, methanol, dimethyl ether, and formic acid.[1−3] Although supported metals are active catalysts for the decomposition of these materials, the reactions with acceptable rates proceed only at higher temperatures.[4−6] Another feature is that CO is also produced in a large quantity; its partial or complete elimination requires the presence of a great amount of H_2O. The catalytic decomposition of formic acid represents an exception, as CO is formed only in very small quantities.[7−11] By means of photolysis the decomposition of the above compounds occurs even at room temperature.[12−15] In the case of the photocatalytic decomposition of formic acid over Au and Pt metals deposited on TiO_2 the formation of CO was completely absent.[16,17]

An interesting feature of the photocatalytic reactions of alcohols is that beside H_2, CO, and CO_2 some other undesired compounds are also formed. In the case of ethanol acetaldehyde is produced, whereas in the photodecomposition and oxidation of methanol a significant amount of methyl formate (MF) was found.[18−24] On TiO_2-supported Pt metals the selectivity of MF fell in the range of 83.1−90.4% and the yields of MF varied between 26.0 and 62.2%.[23] It appears that, due to the effect of illumination, methanol has a very high tendency to be converted into methyl formate. This was well-demonstrated by the results obtained under ultrahigh-vacuum conditions on the TiO_2(110) surface, when the formation of methyl formate was identified even at 200 K.[25,26] The generation of MF was described by the transient formation of CH_3O, HCOH, and HCO surface complexes.

Methyl formate has been considered as a precursor in the synthesis of formamide, dimethyl formamide, acetic acid, propionic acid, cyanhydric acid, and several other materials;[27] therefore, its efficient production represents technological importance. Methyl formate is mainly synthesized by dehydrogenation of methanol over Cu-based catalyst at higher temperatures.[27] In order to know more about the reactivity of MF in the present work, we examine its photocatalytic decomposition over TiO_2 and Pt metals supported by TiO_2. Attempts will be made to decompose methyl formate in visible light using catalysts of smaller bandgap.

2. EXPERIMENTAL SECTION

2.1. Materials. Metal-promoted TiO_2 samples were prepared by impregnating TiO_2 (Hombikat) with the solution of metal compounds to yield a nominal 2 wt % metal. The following compounds of Pt metals were used: $H_2PtCl_6 \cdot 6H_2O$, $Pd(NO_3)_2$, $RhCl_3 \cdot 3H_2O$, H_2IrCl_6, and $RuCl_3 \cdot 3H_2O$. The suspension was dried at 373 K and annealed at 573 K for 1 h. A N-modified TiO_2 sample (named "SX") was also produced following the description of Xu et al.[28] Titanium tetrachloride was used as a precursor. After several steps the NH_3-treated

Received: July 11, 2013
Revised: October 10, 2013
Published: October 10, 2013

 © 2013 American Chemical Society dx.doi.org/10.1021/jp406840n | J. Phys. Chem. C 2013, 117, 22797−22804

Table 1. Characteristic Data for the Catalysts Used

	surface area (m^2/g)	bandgap (eV)	work function of metal (eV)	dispersion of metals (%)
TiO_2 (Hombikat)	200	3.15	~4.6	
TiO_2 (SX)	265	3.02		
TiO_2 + N (SX)	79	1.98		
SiO_2 (Cabosil)	198			
Ir/TiO_2 (Hombikat)			5.76	54
Pt/TiO_2 (Hombikat)			5.70	13
Pd/TiO_2 (Hombikat)			5.12	26
Rh/TiO_2 (Hombikat)			4.98	16
Ru/TiO_2 (Hombikat)			4.71	6

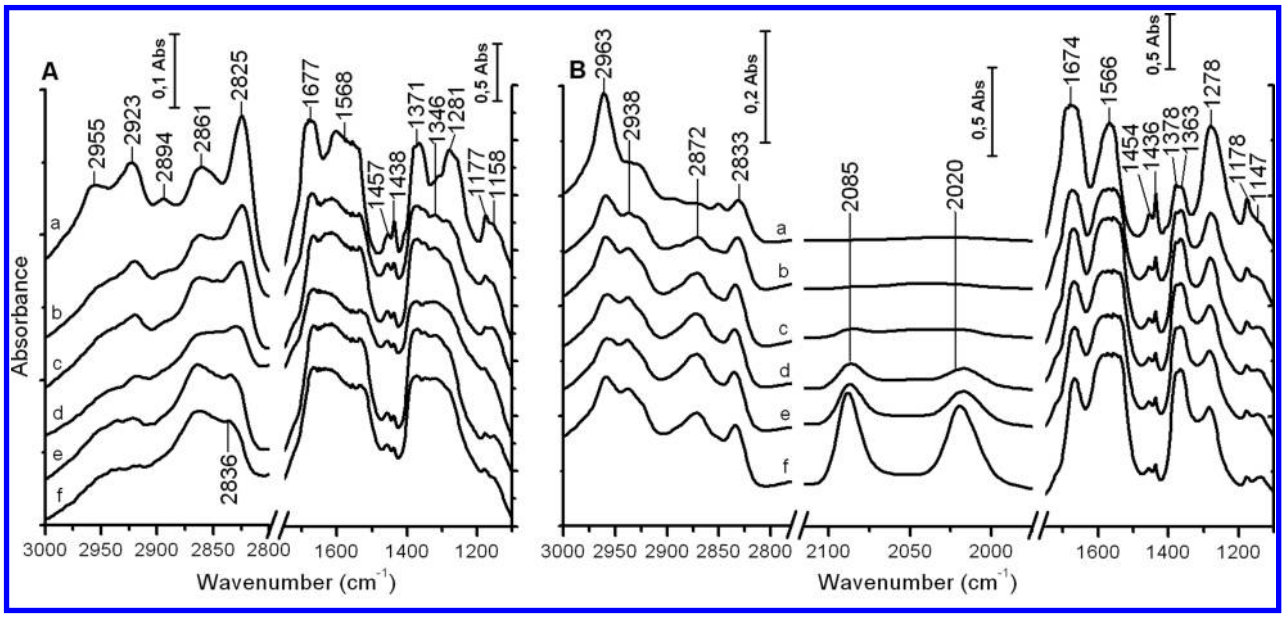

Figure 1. IR spectra of MF as a function of illumination time on TiO_2 and 2% Rh/TiO_2 at 300 K in the presence of ~1.0 Torr of MF for TiO_2 (A) and Rh/TiO_2 (B): (a) 0, (b) 5, (c) 30, (d) 120, (e) 210, and (f) 430 min.

TiO_2 slurry was vacuum-dried at 353 K for 12 h, followed by calcination at 723 K in flowing air for 3 h. For IR studies the dried samples were pressed in self-supporting wafers (30 × 10 mm, ~10 mg/cm^2). For photocatalytic measurements the sample (70−80 mg) was sprayed onto the outer side of the inner quartz tube from aqueous suspension. The surface of the catalyst film was 168 cm^2. The catalysts were oxidized at 573 K and reduced at 573 K in the IR cell or in the catalytic reactor for 1 h. MF was the product of Alfa Aesar, which was stabilized by 3% methanol.

2.2. Methods. For FTIR studies a mobile IR cell housed in a metal chamber was used. The sample can be heated and cooled by 150 K. The IR cell can be evacuated to 10^{-5} Torr using a turbo molecular pumping system. The samples were illuminated by the full arc of a Hg lamp (LPS-220, PTI) outside the IR sample compartment. The IR range of the light was filtered by a quartz tube (10 cm length) filled with triply distilled water applied at the exit of the lamp. The filtered light passed through a high-purity CaF_2 window into the cell. The light of the lamp was focused onto the sample. The output produced by this setting was 300 mW cm^{-2} at a focus of 35 cm. The maximum photon energy at the sample is ca. 5.4 eV. After illumination, the IR cell was moved to its regular position in the IR beam. Infrared spectra were recorded with a Biorad (Digilab Division FTS 155) instrument with a wavenumber accuracy of ±4 cm^{-1}. All of the spectra presented in this study are difference spectra.

For the determination of the bandgap of the solids, diffuse reflectance spectra of TiO_2 samples were obtained using an UV/vis spectro-photometer (Ocean Optics, type USB2000) equipped with a diffuse reflectance accessory.[16,29] The surface areas of the catalysts were determined by Brunauer−Emmett−Teller (BET) method with N_2 adsorption at ~100 K. The dispersion of metals was determined by the adsorption of H_2 at room temperature. Characteristic data for the catalyts are listed in Table 1.

Photocatalytic reaction was followed in the same way as described in our previous paper.[16,23] The photoreactor (volume, 970 mL) consists of two concentric Pyrex glass tubes fitted one into the other and a centrally positioned lamp. It is connected to a gas-mixing unit serving for the adjustment of the composition of the gas or vapor mixtures to be photolyzed in situ. We used a 15 W germicide lamp (type GCL 307T5L/CELL, Lighttech Ltd.), which emits predominantly in the wavelength range of 250−440 nm; its maximum intensity is at 254 nm. For the visible photocatalytic experiments another type of lamp was used (Lighttech GCL 307T5L/GOLD) with 400−640 nm wavelength range and two maximum intensities at 453 and 545 nm. The approximate light intensity at the catalyst films are 3.9 mW/cm^2 for the germicide lamp and 2.1 mW/cm^2 for the other lamp. MF (~5.0%, 1080 μmol) was introduced in

dx.doi.org/10.1021/jp406840n | J. Phys. Chem. C 2013, 117, 22797−22804

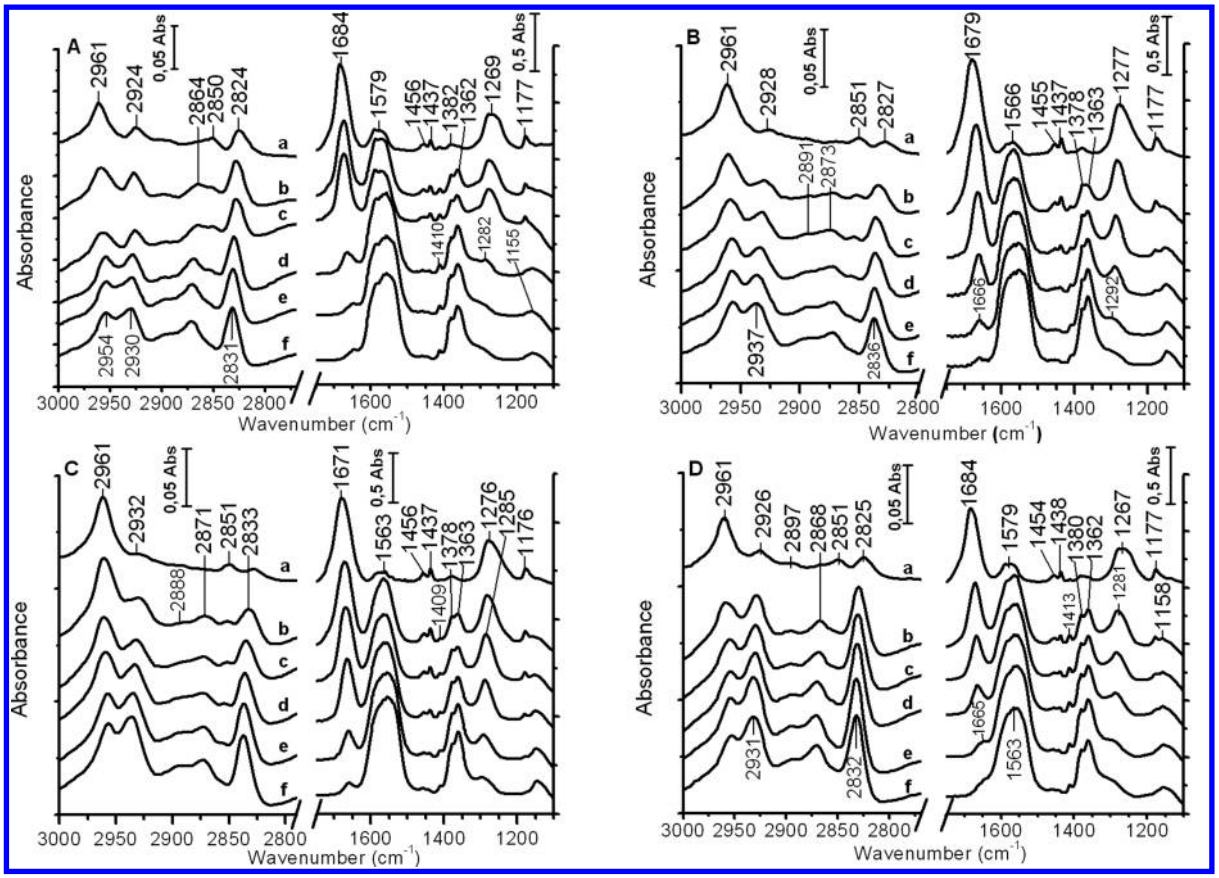

Figure 2. Effects of illumination time on the IR spectra of adsorbed MF on various catalysts at 186−190 K for TiO_2 (A), Pt/TiO_2 (B), Rh/TiO_2 (C), and Pd/TiO_2 (D): (a) 0, (b) 1, (c) 3, (d) 10, (e) 60, and (f) 120 min.

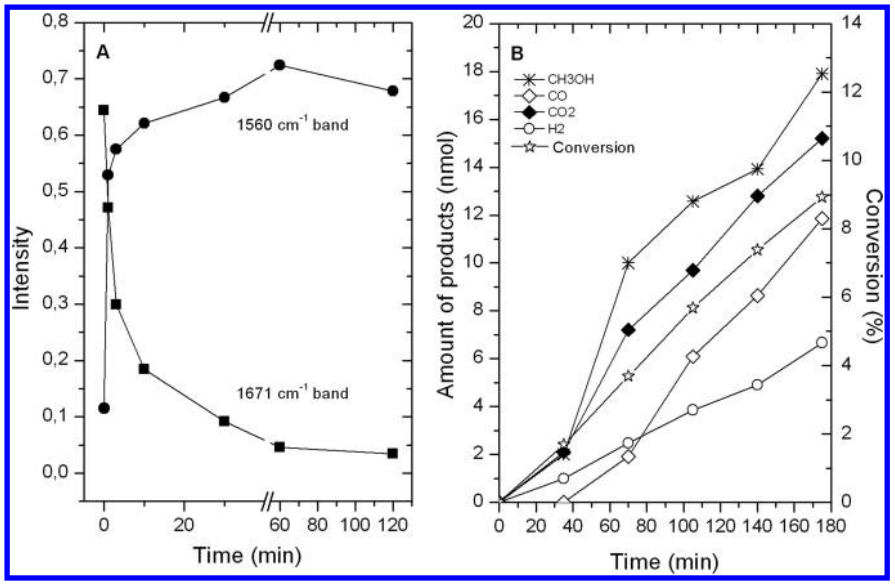

Figure 3. (A) Changes in intensity of the 1671 and 1586 cm^{-1} bands as a function of illumination of adsorbed MF on Rh/TiO_2 at 186 K. (B) Photocatalytic decomposition of MF on TiO_2 at 300 K.

the reactor through an externally heated tube avoiding condensation. The carrier gas was Ar. The gas mixture was circulated by a pump. The reaction products were analyzed with a HP 5890 gas chromatograph equipped with PORAPAK Q and PORAPAK S packed columns. The sampling loop of the GC was 500 μL. The amounts of all products were related to this loop.

3. RESULTS

3.1. Infrared Spectroscopic Study. IR spectra of TiO_2 (Hombikat) in the presence of MF vapor at 300 K showed absorption bands at 2955, 2923, 2894, 2861, and 2825 cm^{-1} in the CH stretching region. Strong bands appeared at 1677, 1568, 1371, and 1281 cm^{-1} and weaker ones at 1457, 1438, 1346, 1177, and 1158 cm^{-1} in the low-frequency range. Illumination

dx.doi.org/10.1021/jp406840n | J. Phys. Chem. C 2013, 117, 22797−22804

Table 2. Vibrational Frequencies (cm^{-1}) of $HCOOCH_3$ Adsorbed on TiO_2 and Rh/TiO_2

TiO_2 at 300 K (from ref 34)	TiO_2 at 300 K (present study)	TiO_2 at 186 K (present study)	Rh/TiO_2 at 300 K (present study)	band assignment
2952	2955	2961	2963	CH_3O
2935			2938	MF
2927	2923	2924		MF
2865	2861	2864	2872	HCOO
2850	2825		2833	CH_3O
1640	1677	1684	1674	MF (νCO)
1575	1568	1579	1566	HCOO (ν_{as})
1406	1438	1437	1436	MF ($\delta_a CH_3$)
1380	1371	1362	1378	HCOO (ν_s)
1281	1281	1269	1278	MF

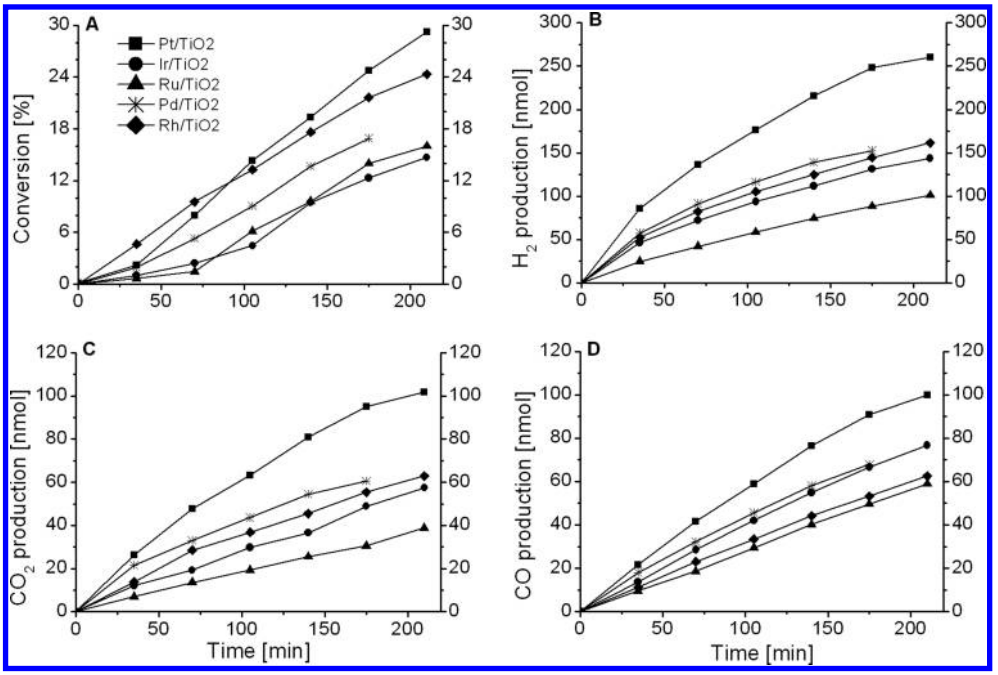

Figure 4. Photocatalytic decomposition of MF on TiO_2 containing various Pt metals: conversion (A), formation of H_2 (B), CO_2 (C), and CO (D).

in MF vapor at 300 K resulted in a slow attenuation of these spectral features. We obtained similar spectra for Rh/TiO_2 catalysts with a slight deviation in the positions of absorption bands. The basic difference was that after 120 min of illumination CO bands appeared at 2085 and 2020 cm^{-1}, the intensity of which further increased with the time of illumination. IR spectra are displayed in Figure 1.

IR spectroscopic measurements were also performed at 186–190 K. In this case MF was adsorbed on the samples at 186–190 K for 30 min and then degassed for 15 min. Spectra obtained on various catalysts are shown in Figure 2. Adsorption of MF on reduced TiO_2 at 186 K produced strong absorption bands at 2961, 2924, 2850, and 2824 cm^{-1} in the CH stretching region. Strong bands appeared at 1684 and 1269 cm^{-1} and weaker ones at 1579, 1456, 1437 1382, (1362), and 1177 cm^{-1} in the low-frequency range. A continuous illumination of the adsorbed layer at 186 K caused only slight spectral changes in the high-frequency range, but resulted in a dramatic alteration in the low-frequency region. The dominant peaks at 1684 and 1269 cm^{-1} attenuated even after short illumination, and at the same time absorption bands at 1579 and 1362 cm^{-1} strengthened. After 10 min of illumination they became the strongest spectral features. We obtained a similar picture on TiO_2 promoted by Pt metals with the difference that CO bands between 2000 and 2100 cm^{-1} also appeared on the IR spectra. In Figure 3A changes in intensities of the absorption bands at 1671 and 1560 cm^{-1} measured on Rh/TiO_2 are plotted. The assignment of absorption bands observed on TiO_2 and Rh/TiO_2 are presented in Table 2.

In order to eliminate the role of TiO_2 IR spectroscopic measurements were carried out with Rh/SiO_2. In this case the adsorption of MF gave an intense band at 1730 cm^{-1}. On the effect of illumination a slow decay was observed in its intensity without the development of any other absorption features. We obtained similar results on pure SiO_2.

3.2. Photocatalytic Measurements. Photocatalytic studies were performed at 300 K. The main products of the photolysis of MF on reduced TiO_2 are CH_3OH, H_2, CO, and CO_2 (Figure 3B). The conversion attained in 180 min of illumination was about 9%. Deposition of Pt metals on TiO_2 increased the conversion of MF and changed the products distribution: H_2, CO, and CO_2 became the main products (Figure 4). The amount of H_2 and CO formed on various catalysts in 210 min are given in Table 3. The activity order of metals was as follows: Pt > Rh=Pd > Ir > Ru. In order to decrease the amount of CO produced in the photoreaction we added H_2O to MF. Results are presented in Figure 5. The addition of H_2O to MF (H_2O/MF ratio of 3:1) enhanced the

dx.doi.org/10.1021/jp406840n | J. Phys. Chem. C 2013, 117, 22797–22804

Table 3. Amounts of H_2 and CO (mol %) Formed on Various M/TiO_2 Catalysts in 210 min

catalyst	H_2	CO
Ir	48.03	25.65
Pt	53.40	20.51
Pd	50.50	23.51
Rh	54.35	21.08
Ru	47.41	27.59

conversion of MF and decreased the CO/H_2 ratio by a factor of 4.

In the following part of the experiments we examined the photoinduced decomposition of MF applying N-doped TiO_2, which was prepared by the method of Xu et al.[28] Some results obtained on Pt/TiO_2 and Pd/TiO_2 are presented in Figure 6. Although these samples exhibited much less photoactivity than those described above, doping TiO_2 with N appreciably increased the extent of photocatalytic decomposition of MF both on the Pt/TiO_2 and Pd/TiO_2 in UV light. The incorporation of N into TiO_2 somewhat decreased the CO/H_2 ratio on both catalysts. An enhanced photocatalytic decomposition was also experienced in visible light, too. This is illustrated by the results of Figure 7.

4. DISCUSSION

4.1. Infrared Spectroscopic Studies. IR spectroscopic measurements have been extensively used for the characterization of the bonding of adsorbed formic acid and MF to different solids including TiO_2.[10,11,30−34] Based on the previous results and interpretation, the absorption band at 1730 cm^{-1} detected after adsorption of MF on Rh/SiO_2 at 300 K corresponds well to the characteristic spectral feature of H-bonded MF. Different IR spectra were obtained on TiO_2 (Figure 2A). The main difference is that the 1725 cm^{-1} band was missing even at 186 K; instead a strong band appeared at 1684 cm^{-1} which can be attributed to the vibration of MF coordinatively bonded to Lewis acid sites of TiO_2.[32−34] In addition, the characteristic spectral features of formate species at 1579 and 1362 cm^{-1} were also identified, indicating that the dissociation of MF to formate proceeded even at ∼186 K. Qualitatively we obtained a similar picture for $metal/TiO_2$ catalysts, which suggests that the dissociation of MF occurs on TiO_2, and the adsorbed species are located on the TiO_2 surface. We could assume the following primary step of the dissociation of MF

$$HCOOCH_{3(a)} = HCOO_{(a)} + CH_{3(a)} \quad (1)$$

Adsorbed CH_3 is characterized by a strong band at 2920 cm^{-1}.[35] Because no such band appeared in the IR spectra of irradiated adsorbed MF, we assume that the CH_3 formed in the primary dissociation process is combined with the surface O of TiO_2 leading to CH_3O species.

$$HCOOCH_3 + O_{(a)} = HCOO_{(a)} + CH_3O_{(a)} \quad (2)$$

The formation of CH_3O is supported by the appearance of the bands at 2824−2827 cm^{-1}.

Continuous illumination of adsorbed MF on TiO_2 at 186 K caused a dramatic spectral change in the low-frequency range: the 1684 cm^{-1} band due to molecularly bonded MF gradually attenuated, while the bands belonging to formate species are strengthened. The presence of Pt metals slightly promotes this process. In addition, absorption bands due to adsorbed CO appeared on the IR spectra of all metal-containing TiO_2 catalysts after extended illumination, indicating the decomposition of adsorbed compounds at the metal/TiO_2 interface. It is remarkable that while in the low-frequency range, dramatic spectral changes occurred as a result of illumination; very little alteration was observed in the high-frequency range.

It is an open question whether MF or formate species exist on metal surfaces. The fact that the adsorption of MF on SiO_2 and Rh/SiO_2 produced only the vibration of weakly adsorbed MF suggests that adsorbed species detected are located on the TiO_2 surface. The formation of CO bands, however, indicates

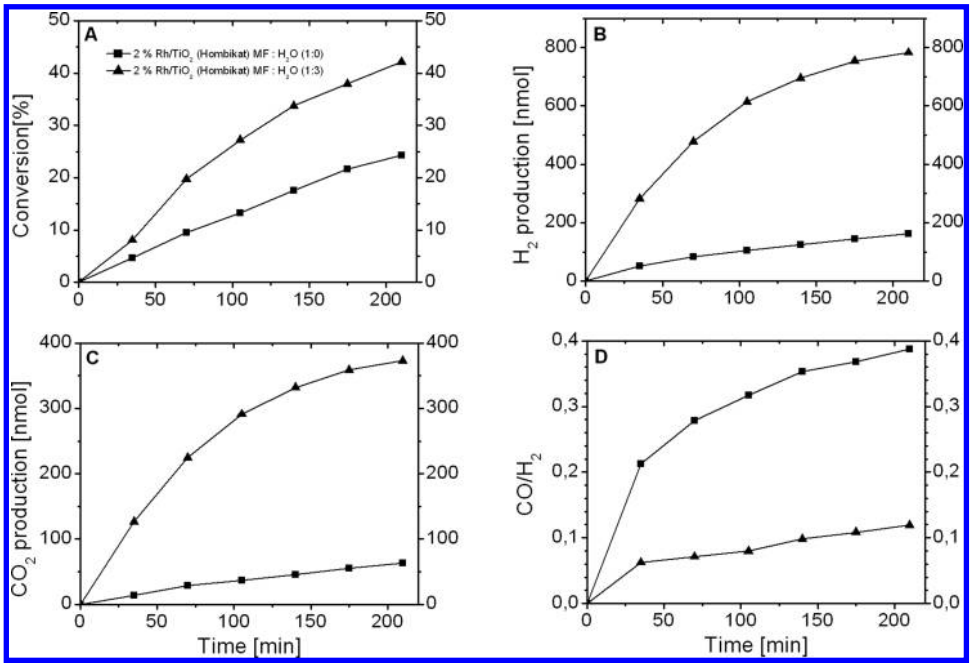

Figure 5. Effects of H_2O addition on the photocatalytic decomposition of MF over Rh/TiO_2 at 300 K.

dx.doi.org/10.1021/jp406840n | J. Phys. Chem. C 2013, 117, 22797−22804

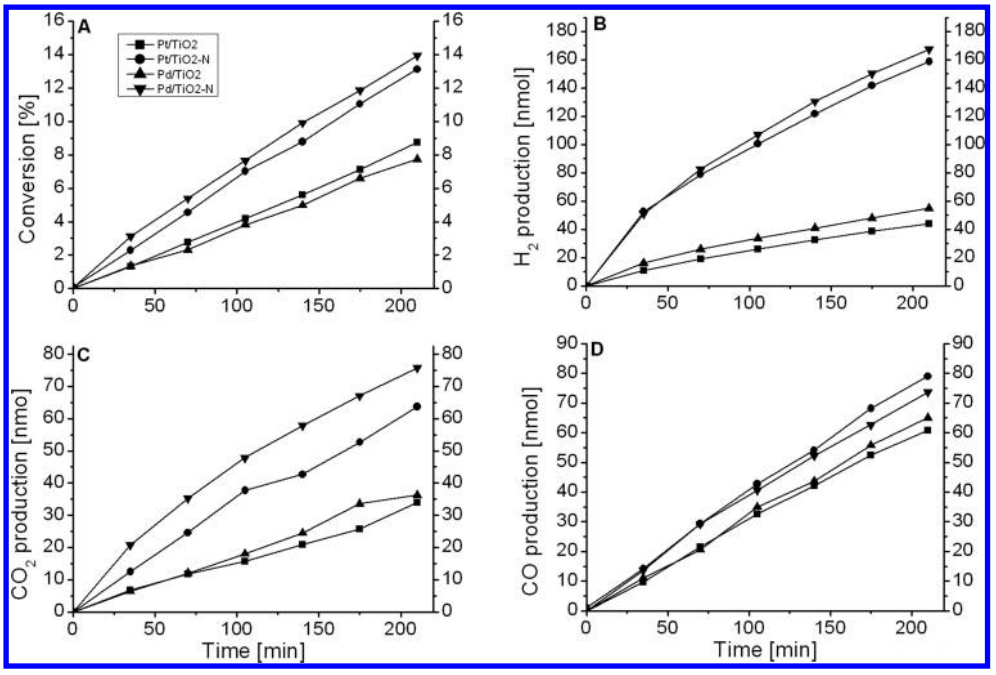

Figure 6. Effects of N-doping of TiO_2 on the photocatalytic decomposition of MF on Pt/TiO_2 and 2% Pd/TiO_2 in UV light.

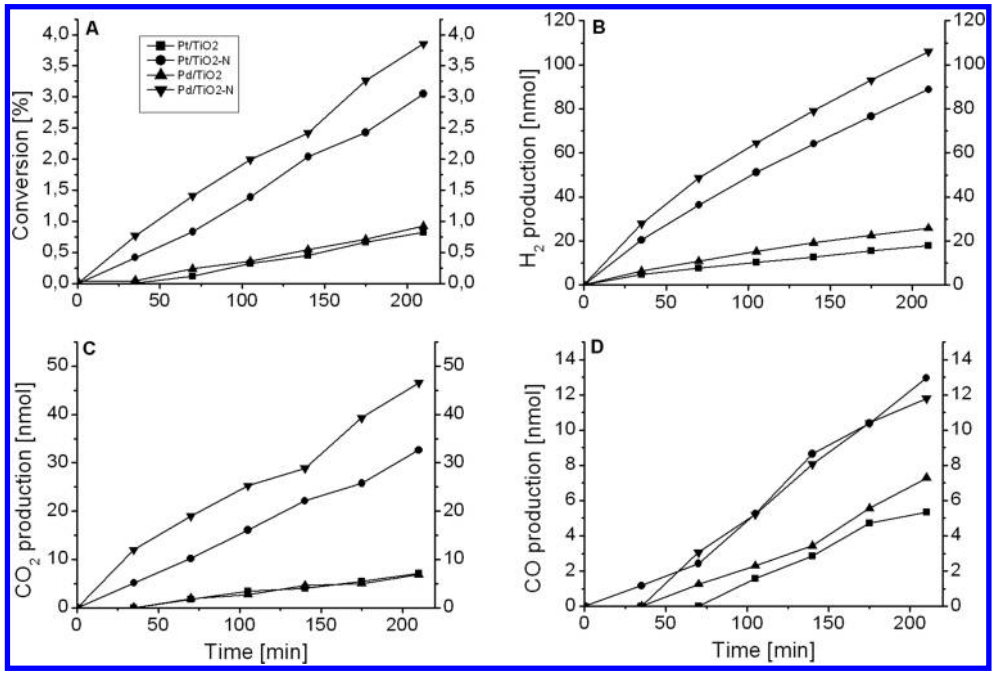

Figure 7. Effects of N-doping of TiO_2 on the photocatalytic decomposition of MF on Pt/TiO_2 and Pd/TiO_2 in visible light.

that the metals can induce the decomposition of adsorbed species very likely at the metal/TiO_2 interface.

4.2. Photocatalytic Decomposition. Results presented suggest that we can count with the occurrence of the following reactions:

$$HCOOCH_3 + OH_{(a)} \rightleftharpoons CH_3O_{(a)} + HCOO_{(a)} + {}^1/_2\, H_{2(g)} \quad (3)$$

$$HCOO_{(a)} \rightleftharpoons CO_{2(g)} + {}^1/_2\, H_{2(g)} \quad (4)$$

$$CH_3O_{(a)} + H_{(a)} \rightleftharpoons CH_3OH_{(g)} \quad (5)$$

$$CH_3O_{(a)} \rightleftharpoons CH_2O_{(a)} + {}^1/_2\, H_{2(g)} \quad (6)$$

$$CH_2O_{(a)} \rightleftharpoons CO_{(g)} + H_{2(g)} \quad (7)$$

The slow rate determining step is very likely the rupture of C–H bond in the formate species, as was proposed for the photoinduced reaction of formic acid.[16,17] The effect of the illumination is attributed to the donation of a photoelectron formed in the photoexcitation process:

$$TiO_2 + h\nu = h^+ + e^- \quad (8)$$

to the formate species

dx.doi.org/10.1021/jp406840n | J. Phys. Chem. C 2013, 117, 22797–22804

$$HCOO_{(a)} + e^- = HCOO_{(a)}{}^{\delta-} \quad (9)$$

This step is followed by the decomposition of formate ion to CO_2 and hydrogen:

$$HCOO_{(a)}{}^{\delta-} = CO_{2(a)}{}^{\delta-} + H_{(a)} \quad (10)$$

$$CO_{2(a)}{}^{\delta-} + h^+ = CO_{2(g)} \quad (11)$$

The presence of CO in the products suggests the occurrence of another reaction, too

$$2HCOO_{(a)}{}^{\delta-} = 2CO_{(a)} + 2OH_{(a)}{}^{\delta-} \quad (12)$$

As was illustrated by the results displayed in Figure 4, the deposition of Pt metals on TiO_2 accelerated the rate of the photocatalytic decomposition of MF, resulting in the formation of H_2, CO_2, and CO. Adding water to MF changed the product distribution: more H_2 and less CO were generated. This feature also appeared in a considerable decrease in the CO/H_2 ratio (Figure 5). The effect of water can be explained by the occurrence of the water-gas shift reaction, which is well-catalyzed by Pt metals.

The promoting effect of metal deposition on TiO_2 has been observed in a number of photoreactions.[13,14] This effect was explained by a better separation of charge carriers induced by illumination and by improved electronic communication between metal particles and TiO_2. We believe that the electronic interaction between the metal and n-type TiO_2 also plays an important role in the enhanced photoactivity of M/TiO_2. Because the work function of TiO_2 (~4.6 eV) is less than that of Pt metals (4.98−5.7 eV), electron transfer may occur from TiO_2 to metals. Metal particles may undergo charge equilibration with TiO_2 and shift the Fermi level of the M/TiO_2 to more negative potentials. The role of such electronic interaction in the activity of TiO_2-supported metals was first established in the case of the decomposition of formic acid on Ni/TiO_2, when TiO_2 was first used as a support.[36] Variation of the work function of TiO_2 doping with altervalent cations influenced the activation energy of the decomposition of formic acid. We assume that the illumination enhances the extent of electron transfer from TiO_2 to metals at the interface of the two solids, leading to an increased rate of photocatalytic reaction. The Schottky barrier at the metal and TiO_2 interface can also function as an efficient barrier preventing electron−hole recombination.[37,38] In the case of gold catalyst Li et al.[39] pointed out that smaller metal particles induce a more negative Fermi level shift than the larger particles.

In the case of the photocatalytic decomposition of formic acid the most active metals possessed the largest work function.[16] On the basis of the conversion data this correlation is valid in the present case, too. Only the low activity of Ir/TiO_2 deviates from this relation. In an attempt to find any correlation between the activity and the size of metal particles one should take into account that CO formed in a reaction can alter the size of metal nanoparticles. As was revealed first by IR spectroscopy[40] and confirmed by scanning tunneling spectroscopy (STM),[41] adsorption of CO can induce structural changes of metal particles. Depending on the reaction temperature, this could be the oxidative disruption or reductive agglomerization of nanoparticles.

It is important to mention that the narrowing of the bandgap of TiO_2 by N incorporation enhanced the activity of M/TiO_2 in the photocatalytic decomposition of methyl formate. This can be also attributed to the prevention of electron−hole recombination. The positive influence of narrowing the bandgap of TiO_2 also appeared in the results obtained in visible light (Figures 6 and 7).

We may compare the photocatalytic decomposition of MF with that of formic acid. There are several features of the photodecomposition of MF which differ from those of formic acid carried out on the same catalysts and under the same experimental conditions.[16] One of them is the considerable amount of CO formed in the photodecomposition of MF. This may mean that the "CH_3" group of MF influences the chemistry of the photoreaction of MF on the catalysts used. We may assume that parallel with the photodecomposition of formate, CH_3O species formed in the primary process (eqs 2 and 3) also decomposes on the effect of illumination, yielding mainly CO (eqs 7 and 12). This process is also enhanced by the illumination through the formation of negatively charged CH_3O.

$$CH_3O_{(a)} + \Theta = CH_3O^{\delta-} \quad (13)$$

We cannot exclude the possibility that photoelectrons activate the molecularly adsorbed MF and induce its decomposition, yielding H_2, CO, and CO_2

$$HCOOCH_3 + \Theta = HCOOCH_3{}^{\delta-} \quad (14)$$

$$HCOOCH_3{}^{\delta-} + O_{(a)} = 2H_2 + CO + CO_2 \quad (15)$$

Another difference is that the photodecomposition of MF on the same M/TiO_2 catalyst is much slower than that of formic acid. A possible reason of this feature is that a fraction of CO is attached to the metals resulting in lowering their promoting effect. Experiments carried out with Rh/TiO_2 saturated with CO confirm this explanation, as it considerably slowed down the photoreaction of MF.

5. CONCLUSION

(i) Illumination of adsorbed MF on pure and Pt metals-containing TiO_2 leads to the dissociation of molecularly adsorbed MF into formate species even at 186 K.

(ii) Pt metals deposited on TiO_2 enhance the rate and the extent of the photocatalytic decomposition of MF, yielding H_2, CO, and CO_2.

(iii) Adding H_2O to MF decreases the amount of CO formed.

(iv) Lowering the bandgap of TiO_2 by N-doping appreciably increased the photocatalytic activity of $metal/TiO_2$ catalysts, and the decomposition of methyl formate was observed even in visible light.

AUTHOR INFORMATION

Corresponding Author

*Fax: +36-62-544-106. E-mail: fsolym@chem.u-szeged.hu.

Notes

The authors declare no competing financial interest.

ACKNOWLEDGMENTS

This work was supported by the grant OTKA under Contract No. K 81517 and TÁMOP under Contract No. 4.2.2.A-11/1/KONV-2012-0047.

REFERENCES

(1) Sandstede, G. In Decomposition of Hydrocarbons into Hydrogen and Carbon for the CO_2-Free Production of Hydrogen. *Proceedings of the Ninth World Hydrogen Energy Conference*, Paris, France; Veziroglu, T. N., Derive, C., Pottier, J., Eds.; 1992; p 1745.

(2) Haryanto, A.; Fernando, S.; Murali, N.; Adhikari, S. Current Status of Hydrogen Production Techniques by Steam Reforming of Ethanol: A Review. *Energy Fuels* **2005**, *19*, 2098−2106.

(3) Brown, L. F. A Comparative Study of Fuels for On-Board Hydrogen Production for Fuel-Cell-Powered Automobiles. *Int. J. Hydrogen Energy* **2001**, *26*, 381−397.

(4) Mavrikakis, M.; Barteau, M. A. Oxygenate Reaction Pathways on Transition Metal Surfaces. *J. Mol. Catal. A: Chem.* **1998**, *131*, 135−147.

(5) Dickinson, A.; James, D.; Perkins, N.; Cassidy, T.; Bowker, M. The Photocatalytic Reforming of Methanol. *J. Mol. Catal. A: Chem.* **1999**, *146*, 211−221.

(6) Díagne, C.; Idriss, H.; Kiennemann, A. Hydrogen Production by Ethanol Reforming over Rh/CeO_2−ZrO_2 Catalysts. *Catal. Commun.* **2002**, *3*, 565−571.

(7) Ojeda, M.; Iglesia, E. Formic Acid Dehydrogenation on Au-Based Catalysts at Near-Ambient Temperatures. *Angew. Chem., Int. Ed.* **2009**, *48*, 4800−4803.

(8) Koós, Á.; Solymosi, F. Production of CO-Free H_2 by Formic Acid Decomposition over Mo_2C/Carbon Catalysts. *Catal. Lett.* **2010**, *138*, 23−27.

(9) Bulushev, D. A.; Beloshapkin, S.; Ross, J. R. H. Hydrogen from Formic Acid Decomposition over Pd and Au Catalysts. *Catal. Today* **2010**, *154*, 7−12.

(10) Gazsi, A.; Bánsági, T.; Solymosi, F. Decomposition and Reforming of Formic Acid on Supported Au Catalysts: Production of CO-Free H_2. *J. Phys. Chem. C* **2011**, *115*, 15459−15466.

(11) Solymosi, F.; Koós, Á.; Liliom, N.; Ugrai, I. Production of CO-Free H_2 from Formic Acid. A Comparative Study of the Catalytic Behavior of Pt Metals on a Carbon Support. *J. Catal.* **2011**, *279*, 213−219.

(12) Hoffmann, M. R.; Martin, S. T.; Choi, W.; Bahnemann, D. W. Environmental Applications of Semiconductor Photocatalysis. *Chem. Rev.* **1995**, *95*, 69−96.

(13) Linsebigler, A.; Lu, G.; Yates, J. T., Jr. Photocatalysis on TiO_2 Surfaces: Principles, Mechanisms, and Selected Results. *Chem. Rev.* **1995**, *95*, 735−758.

(14) Connelly, K.; Wahab, A. K.; Idriss, H. Photoreaction of Au/TiO_2 for Hydrogen Production from Renewables: A Review on the Synergistic Effect between Anatase and Rutile Phases of TiO_2. *Mater. Renewable Sustainable Energy* **2012**, *1*, 3.

(15) Halasi, Gy.; Ugrai, I.; Solymosi, F. Photocatalytic Decomposition of Ethanol on TiO_2 Modified by N and Promoted by Metals. *J. Catal.* **2011**, *281*, 309−317.

(16) Halasi, Gy.; Schubert, G.; Solymosi, F. Photodecomposition of Formic Acid on N-Doped and Metal-Promoted TiO_2. Production of CO-Free H_2. *J. Phys. Chem. C* **2012**, *116*, 15396−15405.

(17) Gazsi, A.; Schubert, G.; Pusztai, P.; Solymosi, F. Photocatalytic Decomposition of Formic Acid and Methyl Formate on TiO_2 Doped with N and Promoted with Au. Production of H_2. *Int. J. Hydrogen Energy* **2013**, *38*, 7756−7766.

(18) Chuang, C.-C.; Chen, C.-C.; Lin, J.-L. Photochemistry of Methanol and Methoxy Groups Adsorbed on Powdered TiO_2. *J. Phys. Chem. B* **1999**, *103*, 2439−2444.

(19) Wu, W.-C.; Chuang, C.-C.; Lin, J.-L. Bonding Geometry and Reactivity of Methoxy and Ethoxy Groups Adsorbed on Powdered TiO_2. *J. Phys. Chem. B* **2000**, *104*, 8719−8724.

(20) Araña, J.; Doña-Rodríguez, J. M.; Garriga, C.; González-Díaz, O.; Herrera-Melián, J. A.; Pérez, J. FTIR Study of Gas-Phase Alcohols Photocatalytic Degradation with TiO_2 and AC-TiO_2. *Appl. Catal., B* **2004**, *53*, 221−232.

(21) Chiarello, G. L.; Aguirre, M. H.; Selli, E. Hydrogen Production by Photocatalytic Steam Reforming of Methanol on Noble Metal-Modified TiO_2. *J. Catal.* **2010**, *273*, 182−190.

(22) Kominami, H.; Sugahara, H.; Hashimoto, K. Photocatalytic Selective Oxidation of Methanol to Methyl Formate in Gas Phase over Titanium(IV) Oxide in A Flow-Type Reactor. *Catal. Commun.* **2010**, *11*, 426−429.

(23) Halasi, Gy.; Schubert, G.; Solymosi, F. Comparative Study on the Photocatalytic Decomposition of Methanol on TiO_2 Modified by N and Promoted by Metals. *J. Catal.* **2012**, *294*, 199−206.

(24) Huang, X.; Cant, N. W.; Wainwright, M. S.; Ma, L. The Dehydrogenation of Methanol to Methyl Formate: Part I: Kinetic Studies Using Copper-Based Catalysts. *Chem. Eng. Proc.* **2005**, *44*, 393−402.

(25) Phillips, K. R.; Jensen, S. C.; Baron, M.; Li, S.-C.; Friend, C. M. Sequential Photo-Oxidation of Methanol to Methyl Formate on TiO_2(110). *J. Am. Chem. Soc.* **2013**, *135*, 574−577.

(26) Xu, B.; Liu, X.; Haubrich, J.; Madix, R. J.; Friend, C. M. Selectivity Control in Gold-Mediated Esterification of Methanol. *Angew. Chem., Int. Ed.* **2009**, *48*, 4206−4209.

(27) Jenner, G. Homogeneous Catalytic Reactions Involving Methyl Formate. *Appl. Catal., A* **1995**, *121*, 25−44.

(28) Xu, J.-H.; Dai, W.-L.; Li, J.; Cao, Y.; Li, H.; He, H.; Fan, K. Simple Fabrication of Thermally Stable Apertured N-Doped TiO_2 Microtubes as a Highly Efficient Photocatalyst under Visible Light Irradiation. *Catal. Commun.* **2008**, *9*, 146−152.

(29) Beranek, R.; Kisch, H. Tuning the Optical and Photoelectrochemical Properties of Surface-Modified TiO_2. *Photochem. Photobiol. Sci.* **2008**, *7*, 40−48.

(30) Forzatti, P.; Tronconi, E.; Busca, G.; Tittarelli, P. Oxidation of Methanol to Methyl Formate over V-Ti Oxide Catalysts. *Catal. Today* **1987**, *1*, 209−218.

(31) Busca, G.; Elmi, A. S.; Forzatti, P. Mechanism of Selective Methanol Oxidation over Vanadium Oxide−Titanium Oxide Catalysts: A FT-IR and Flow Reactor Study. *J. Phys. Chem.* **1987**, *91*, 5263−5269.

(32) Chuang, C.-C.; Wu, W.-C.; Huang, M.-C.; Huang, I.-C.; Lin, J.-L. FTIR Study of Adsorption and Reactions of Methyl Formate on Powdered TiO_2. *J. Catal.* **1999**, *185*, 423−434.

(33) Popova, G. Y.; Andrushkevich, T. V.; Chesalov, Y. A.; Stoyanov, E. S. In Situ FTIR Study of the Adsorption of Formaldehyde, Formic Acid, and Methyl Formiate at the Surface of TiO_2 (Anatase). *Kinet. Catal.* **2000**, *41*, 885−891.

(34) Lukaski, A. C.; Muggli, D. S. Photocatalytic Oxidation of Methyl Formate on TiO_2: A Transient DRIFTS Study. *J. Catal.* **2004**, *223*, 250−261.

(35) Solymosi, F.; Klivényi, G. HREELS Study of CH_3I and CH_3 Adsorbed on Rh(111) Surface. *J. Electron Spectrosc. Relat. Phenom.* **1993**, *64/65*, 499−506.

(36) Solymosi, F. Importance of the Electric Properties of Supports in the Carrier Effect. *Catal. Rev.* **1968**, *1*, 233−255.

(37) Ismail, A. A.; Bahnemann, D. W.; Bannat, I.; Wark, M. Gold Nanoparticles on Mesoporous Interparticle Networks of Titanium Dioxide Nanocrystals for Enhanced Photonic Efficiencies. *J. Phys. Chem. C* **2009**, *113*, 7429−7435.

(38) Alvaro, M.; Cojocaru, B.; Ismail, A. A.; Petrea, N.; Ferrer, B.; Harraz, F. A.; Parvulescu, V. I.; Garcia, H. Visible-Light Photocatalytic Activity of Gold Nanoparticles Supported on Template-Synthesized Mesoporous Titania for the Decontamination of the Chemical Warfare Agent Soman. *Appl. Catal., B* **2010**, *99*, 191−197.

(39) Wu, G.; Chen, T.; Su, W.; Zhou, G.; Zong, X.; Lei, Z.; Li, C. H_2 Production with Ultra-Low CO Selectivity via Photocatalytic Reforming of Methanol on Au/TiO_2 Catalyst. *Int. J. Hydrogen Energy* **2008**, *33*, 1243−1251.

(40) Solymosi, F.; Pásztor, M. An Infrared Study of the Influence of CO Chemisorption on the Topology of Supported Rhodium. *J. Phys. Chem.* **1985**, *89*, 4789−4793.

(41) Berkó, A.; Ménesi, G.; Solymosi, F. Scanning Tunneling Microscopy Study of the CO-Induced Structural Changes of Rh Crystallites Supported by TiO_2(110). *J. Phys. Chem.* **1996**, *100*, 17732−17734.